A theoretical spectroscopy study of the X3Sigma- and the A3Pi states of the C2S radical

Riccardo Tarroni, Stuart Carter, Nicholas C. Handy

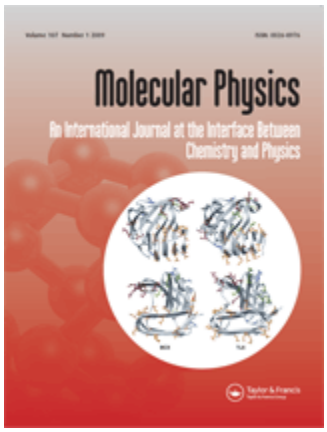

A theoretical spectroscopy study of the X3Sigma- and the A3Pi states of the C2S radical

Journal:	*Molecular Physics*
Manuscript ID:	TMPH-2007-0002
Manuscript Type:	Full Paper
Date Submitted by the Author:	04-Jan-2007
Complete List of Authors:	Tarroni, Riccardo; Università di Bologna, Dipartimento di Chimica Fisica ed Inorganica Carter, Stuart; University of Reading Handy, Nicholas C.; University of Cambridge, Chemistry
Keywords:	vibronic interaction, triplets, triatomic radicals, energy levels, theoretical spectroscopy
Note: The following files were submitted by the author for peer review, but cannot be converted to PDF. You must view these files (e.g. movies) online.	
ccs_paper_v2.tex	

A theoretical spectroscopy study of the $X^3\Sigma^-$ and the $A^3\Pi$ states of the C_2S radical

Riccardo Tarroni *†
Dipartimento di Chimica Fisica ed Inorganica,
Università di Bologna, 40136 Bologna, Italy

Stuart Carter
Department of Chemistry, University of Reading
Reading RG6 2AD, United Kingdom

Nicholas C. Handy
Department of Chemistry, University of Cambridge,
Lensfield Road, Cambridge CB2 1EW, United Kingdom

January 3, 2007

Abstract

The spin-rovibronic levels for the $X^3\Sigma^-, A^3\Pi$ electronic system of C_2S are calculated variationally, using *ab initio* potential energy surfaces and taking into account the non-adiabatic coupling between the two states. The energies of selected levels with Σ and Π vibronic symmetry, up to ~ 16500 cm^{-1}, are reported and compared with available experimental data.

*Corresponding author
†E-mail: riccardo.tarroni@unibo.it, Phone: +39-051-6446754, Fax: +39-051-2093690

1 Introduction

The C_2S radical has been extensively studied using pure rotational spectroscopy techniques [1, 2, 3, 4], because of its importance in astrophysics as a velocity, density and age molecular probe of dark celestial bodies (see e.g. [5, 6] and references therein). The electronic ground state of this radical has $^3\Sigma^-$ symmetry. Its vibrational spectrum has been studied both in rare-gas matrices [7, 8, 9] and in the gas phase using laser induced fluorescence (LIF) techniques [10]. The first excited electronic state, of $^3\Pi$ symmetry, has been recently investigated both in the gas phase, using LIF techniques, [10, 11] and in rare gas matrices [12].

Most theoretical studies deal with the ground state of C_2S and other C_nS thiocumulenes or C_nS_2 clusters [13, 14, 15, 16]. However some intermediate level computations on excited states of C_2S appeared in the literature immediately after its experimental detection [17, 18] and recently have also accompanied experimental papers [11, 12].

In Ref. [12] the electronic structure of the radical was studied in detail and a conical intersection between the ground $X^3\Sigma^-$ and the $A^3\Pi$ was located at a CC bond length of ~ 1.22 Å. This intersection produces an avoided crossing, for bent geometries, between the $X^3\Sigma^-(1^3A'')$ state and the $2^3A''$ component of the $A^3\Pi$ state, which may be responsible for the perturbations detected in the highest vibrational levels of the $A^3\Pi$ state [11]. This effect adds to the well known Renner-Teller interaction between the $1^3A'$ and the $2^3A''$ components of the $A^3\Pi$ state [19, 20], caused by their degeneracy at linear geometries. In other words, the $X^3\Sigma^-, A^3\Pi$ system of C_2S represents a case of three-state vibronic interaction.

This kind of complex interaction has been extensively studied in triatomic radicals by our research group; however only doublet states have been considered to date [21, 22, 23, 24, 25, 26, 27, 28]. On the other hand, we have recently extended the variational theory of triatomic radicals to cover also triplets [29], but in the first application, the C_2O radical, the ground $X^3\Sigma^-$ and first excited $A^3\Pi$ states were considered as uncoupled.

In this paper we undertake a detailed theoretical spectroscopy study of the $X^3\Sigma^-$ and $A^3\Pi$ states of C_2S, taking explicitly into account their non-adiabatic coupling. This represents the first application of the triplet's theory outlined in Ref.[29] to a three-state vibronic interaction.

2 Computational methodologies

2.1 Diabatic Potential Energy Surfaces

The *ab initio* computations needed to obtain the adiabatic energies of the $X^3\Sigma^-(1A'')$ and of the doubly degenerate $A^3\Pi(2A'', 1A')$ electronic states have been performed using the MOLPRO code [30]. The three electronic surfaces have been mapped at 215 geometries (first set) close to the minima of the three states, for $2.0 \leq R_{CC} \leq 3.0$ bohr, $2.6 \leq R_{CS} \leq 3.7$ bohr and $180 \geq \widehat{\mathrm{CCS}} \geq 130$ degree, using the Internally Contracted Multi Reference Configuration Interaction (ICMRCI) method [31, 32] and the cc-pVQZ basis set [33].

The diabatic molecular orbitals orbitals [34] and the reference configurations were obtained from state-averaged full-valence CASSCF computations [35, 36] including the lowest two triplet states of A'' symmetry and the lowest triplet state of A' symmetry. To keep computations to a manageable size, only configurations having a weight greater than 0.01 were included in the ICMRCI step. However, to improve the quality of the stretching part of the final potential energy surfaces, ICMRCI computations were repeated for the 55 linear geometries (second set), using C_{2v} symmetry and a threshold of 0.001 in the selection of reference configurations.

The energies obtained from the first set of computations, including both linear and bent geometries, were diabatized according to the method of Pacher et al. [37, 38] (see also Ref.[21] for more details) and then fitted to symmetry restricted polynomial expansions in the stretching and bending coordinates, using the SURFIT [39] program and following a well tested procedure (see e.g. Ref.[21]). The energies obtained from the second set of computations, including only linear geometries, were fitted to a polynomial expansion in the stretching coordinates only and the resulting coefficients were then substituted to those obtained from the first set. The coefficients of the resulting $V_{\Sigma^-}, V_{\Pi^-}, V_{\Pi^+}$ and V_{12} diabatic surfaces are listed in Table 1. The equilibrium geometries we found are $R_{CC}^{eq} = 1.3194$ Å, $R_{CS}^{eq} = 1.5720$ Å for the $X^3\Sigma^-$ state and $R_{CC}^{eq} = 1.2471$ Å, $R_{CS}^{eq} = 1.6167$ Å for the $A^3\Pi$ state, in good agreement both with previous computational works [17, 18, 13, 12] and with experiment [2].

In previous works on vibronically-coupled three-state systems [21, 22, 23, 24, 25, 26, 27, 28] we found that the $\Sigma - \Pi$ energy separation T_e (corresponding to the $C_{000}^{\Pi^-}$ and $C_{000}^{\Pi^+}$ coefficients of the V_{Π^-}, V_{Π^+} surfaces) and the C_{000}^{12} coefficient of the V_{12} diabatic

coupling surface are crucial parameters to obtain accurate coupled diabatic surfaces. In the present work we had to slightly adjust T_e from 0.041665 to 0.04090 E_h (8977 cm^{-1}), and C_{000}^{12} from 0.046799 to 0.0471 E_h, in order to better reproduce the main features of the experimental spectrum [11].

The contour plots of the diabatic surfaces for linear geometries is reported in Figure 1. The crossing seam shown in the same figure is about 15300 cm^{-1} and 6300 cm^{-1} above the minima of the $X^3\Sigma^-$ and $A^3\Pi$ states, respectively. It is located at $R_{CC} \approx 1.14$ Å, hence at a shorter distance compared to that reported in Ref.[12]. While the crossing can be safely neglected to describe the vibrational levels of the $X^3\Sigma^-$ state and the lowest vibronic levels of the $A^3\Pi$ state, it can not be ignored to accurately describe the highest energy part of the $A^3\Pi$ rovibronic structure

2.2 Vibronic energy levels

Vibronic levels for the most abundant $^{12}C^{12}C^{32}S$ isotopomer were calculated up to a total angular momentum $J = 3$, by means of the variational program RVIB3, which is fully discussed in Refs.[21, 26]. The code includes recent developments to handle also triplets [29].

To establish a direct connection with experiment [11] we calculated states up to ∼16500 cm^{-1} above the minimum of the $X^3\Sigma^-$ state. A careful choice of the basis was then mandatory, in order to obtain converged results with matrices of manageable size. To improve convergence, the one dimensional stretching basis was built using the following combination of pure q_{CC} and q_{CS} stretching modes:

$$Q_1 = -0.876226\ q_{CC} + 0.481901\ q_{CS} \quad (1)$$

$$Q_3 = 0.567249\ q_{CC} + 0.823546\ q_{CS} \quad (2)$$

These are the normal coordinates resulting from the diagonalization of the **GF** Wilson matrix for the $X^3\Sigma^-$ state, as calculated by means of the SURFIT code. The above coefficients indicate that the Q_1 and Q_3 coordinates are mostly CC and CS stretching, respectively.

The rovibrational basis set for stretching modes was set up from 25 one-dimensional harmonic oscillators, contracted to 30 two-dimensional functions, and, for the bending mode, from 35 associated Legendre functions contracted to 25. This basis ensures converged results even for higher levels with a dominant "Π" character, but not for

levels of the same energy with a dominant "Σ" character. This, however, is a minor problem since we are not interested in highly excited levels of the $X^3\Sigma^-$ state. With this choice of the basis, the size of matrices to be diagonalized in the full ro-vibronic analysis is 17600.

The phenomenological spin-orbit parameter A_{SO} for the $A^3\Pi$ state was empirically set to -135.0 cm^{-1}, in order to best reproduce the experimental separation of the Π_0, Π_1, Π_2 sub-levels of the $A^3\Pi(100)$ state [11]. The spin-spin coupling constant was set to zero, because the rotational structure of the vibronic bands is outside the scope of the present work.

3 Discussion

Due to the quite large value of T_e, levels with a dominant "Π" contribution to the wavefunction, hence unambiguously belonging to the $A^3\Pi$ excited state, start appearing above 9000 cm^{-1}. The number of levels at and above this energy is very high, as clearly shown in Figure 2. In fact there exist ∼44500 spin-rovibronic levels, below 16000 cm^{-1} and with $J \leq 3$, hence "Π" levels are intrinsically difficult to be located and identified, especially when accidental near-degeneracies lead to a mixing with highly vibrationally excited levels of the $X^3\Sigma^-$ state. To identify the "Π" levels and to assign them in terms of v_1, v_2, v_3 quantum numbers, we then combined the examination of the variational coefficients to the plotting of the vibrational part of the wavefunctions.

In vibronically-coupled electronic systems, like the $X^2\Sigma^+$, $A^2\Pi$ states of C_2H, HCN^+ and C_2Cl, the assignment of the levels is often very difficult and ambiguous, if ever possible. In these cases, the only quantum number which can be definitely used is the sum K between vibrational and electronic angular momenta. Fortunately, for C_2S the coupling between the two states is not strong, due to the larger value of T_e, hence assignments in terms of the v_1, v_2, v_3 quantum numbers proved to be quite straightforward.

In Table 2 and Table 3 we report a selection of the calculated energy levels of the $X^3\Sigma^-$ and the $A^2\Pi$ states, respectively. Only levels with $v_1 + v_2 + v_3 \leq 4$ and $K \leq 1$ ($\Sigma_0, \Sigma_1, \Pi_0, \Pi_1, \Pi_2$ levels) are reported, because they are the most easily experimentally detectable.

For the $X^3\Sigma^-$ state, the comparison with experiment [10] is straightforward. The

root mean square deviation between calculated and experimental value is 14.2 cm^{-1}, which can be considered fairly good since it has been obtained using coupled diabatic surfaces. For all the examined levels the contribution of the $X^3\Sigma^-$ to the total wavefunction ("Σ" character) is greater than 0.9, indicating that their electronic character is essentially pure.

For the $A^3\Pi$ state the comparison with experiment is, for several reasons, more difficult. First, due to the Renner-Teller and the spin-orbit couplings, each vibrational term splits into many levels [19, 20], giving an intrinsically more dense spectrum. In addition, we found that some of these are further split by local interactions with accidentally degenerate high-lying levels of the $X^3\Sigma^-$ system (see, e.g. the $(010)\kappa^3\Sigma_1$ level in Figure 2, or the $(110)\kappa^3\Sigma_0$ in Table 3). Second, experimental data are far from complete and extend over several thousands of wavenumbers [11]. Finally, most of the observed bands are yet unassigned and only the overall symmetry, deduced from the rotational structure, is known [11].

In Table 3 we tried to match our predicted spectrum with available experimental data [10, 11, 12]. The comparison proved to be quite involved, because of the lack of several important pieces of experimental information, regarding in particular the sublevels of the (001) and (010) states. This information, whenever available, will provide a clearer test of the overall accuracy of our theoretical potentials.

As pointed out in the previous section, our diabatic surfaces were slightly adjusted, and the A_{SO} effective spin-orbit splitting was chosen to best reproduce the Π_0, Π_1, Π_2 sub-levels of the (100) state. So, it is not surprising that the $(v_1 00)$ progression (bands labeled as "$A, B, C, N, R, W, AH, AI, AJ, AR$" in Ref.[11]) and the (000) state [12] are well reproduced.

However, the prediction of the $(v_1 10)$ progression (bands "$F, G, Y, Z, AA, AB, AK, AL, AM, AO$" [11]) is less satisfactory, with a maximum deviation of +70 cm^{-1} in the calculated energy of the $(110)\kappa^3\Sigma_1$ level, indicating that the bending part of the potential needs substantial improvements.

With this in mind, we tried to assign the remaining bands observed in the gas phase; fortunately, for these, the vibronic symmetries deduced from the rotational structure are available.

In Figure 3 we compare our calculated energies with the observed band origins, grouping the data according to the vibronic symmetry. It is evident that in the observed

spectrum there is an excess of levels with Π_1 symmetry, compared to Π_0 and Π_2. The lack of Π_2 bands may be due to their overall smaller intensity. Π_0 bands, on the other hand, have generally an intensity comparable to the Π_1 bands. We suspect that the reduced number of the former compared to the latter may be due to the lack of the observation, in some cases, of the $J = 1 - 0$ transition. In other words, some Π_0 bands might have been mis-assigned as Π_1.

In the experimental gas-phase spectrum[11] there remain two unassigned bands of Σ symmetry. For one of these, observed at 11655.5 cm^{-1} (band "H"), the most suitable assignment seems to be $(050)\kappa^3\Sigma_0$, (calculated at 11733 cm^{-1}). The second, observed at 12331.4 cm^{-1} (band "M"), falls between the predicted energies for the $(130)\mu^3\Sigma_0$ and the $(111)\kappa^3\Sigma_0$. We lean to the second possibility, because our potential tends to overestimate levels with bending excitations.

Turning our attention to the remaining Π states, we tried to find out some bands which might be attributed to the $(00v_3)$ or to the $(10v_3)$ progressions. Having assigned the band "M" as $(111)\kappa^3\Sigma_0$, it is reasonable that some of the sub-bands of the (101) state should be visible. The bands observed at 11858.8 cm^{-1} (band "J") and at 11983.6 cm^{-1} (band "K") are fairly close to the predicted energies for the $(101)^3\Pi_1$ and the $(101)^3\Pi_0$ levels, respectively, but they are classified as Π_2 and Π_1 in Ref.[11]. Our assignment is then based on the hypothesis of a partial misinterpretation of the vibronic symmetry. Here and in similar cases, a question mark is put in the corresponding entry of Table 3.

Other bands which may be attributed as $(v_1 0 v_3)$ bands are those observed at 11452.8 cm^{-1} (band "E"), 11716.8 cm^{-1} (band "I"), 12770.3 cm^{-1} (band "O"), 13535.2 cm^{-1} (band "AC"), 13671.9 cm^{-1} (band "AE"), 13802.9 cm^{-1} (band "AF"), 15318.3 cm^{-1} (band "AP"), and 15475.5 cm^{-1} (band "AQ"), which may be assigned as $(003)^3\Pi_2$, $(003)^3\Pi_0$, $(102)^3\Pi_0$, $(201)^3\Pi_2$, $(201)^3\Pi_1$, $(201)^3\Pi_0$, $(301)^3\Pi_2$ and $(301)^3\Pi_1$, respectively.

Some of the remaining Π bands have been assigned to levels with bending excitation. These are the bands at 11278.4 cm^{-1} (band "D"), 12001.1 cm^{-1} (band "L"), 12814.6 cm^{-1} (band "P") and 12907.8 cm^{-1} (band "T"") which may be assigned as $(040)\kappa^3\Pi_0$, $(120)\kappa^3\Pi_1$, $(121)\kappa^3\Pi_1$ and $(121)\kappa^3\Pi_0$, respectively.

The remaining six bands, labeled as "Q, S, U, V, AD, AN", were left unassigned. These may be extra states with "Σ" electronic character, gaining intensity through the vibronic interaction.

4 Conclusions

The $X^3\Sigma^-$ and $A^3\Pi$ states of the CCS have been studied theoretically, using variational techniques and *ab initio* diabatic potential energy surfaces. All experimentally known levels of the $X^3\Sigma^-$ state are readily reproduced. For the $A^3\Pi$ state the interpretation of the experimental data proved to be more difficult. That was mainly due to the intrinsically greater complexity of the observed spectrum, which is characterized by a medium-small vibronic interaction on top of a Renner-Teller interaction, and to some inaccuracies in the bending part of our *ab initio* potentials.

In summary, we believe that the overall results of our theoretical analysis are nevertheless very satisfactory, considering the amount of difficulties concentrated in a single problem. Our contribution aims to be a first step toward a full understanding of the present experiments and a stimulus for other studies on this challenging molecule.

5 Acknowledgments

This work was supported by the MIUR of Italy, the University of Bologna and the US Office of Naval Research (grant No. N00014-01-1-0235). Part of this work has been performed (by SC) under the Project HPC-EUROPA (R113-CT-2003-506079), with the support of the European Community - Research Infrastructure Action under the FP6 "Structuring the European Research Area" Programme. R. T. would like to acknowledge P. J. Knowles and H. -J. Werner for providing him with access to the MOLPRO code.

References

[1] S. Saito, K. Kawaguki, S. Yamamoto, M. Ohishi, H. Suzuki, and N. Kaifu, Astrophys. J. **317**, L115 (1987).

[2] S. Yamamoto, S. Saito, K. Kawaguki, Y. Chicada, H. Suzuki, N. Kaifu, S. Ishikawa and M. Ohishi, Astrophys. J. **361**, 318 (1990).

[3] M. Ikeda, Y. Sekimoto and S. Yamamoto, J. Mol. Spectrosc. **185**, 21 (1997).

[4] H. Shinnaga and S. Yamamoto, Astrophys. J. **544**, 330 (2000).

[5] W. D. Langer, T. Velusamy, T. B. H. Kuiper, S. Levin, E. Olsen and V.Migenes, Astrophys. J. **453**, 293 (1995).

[6] I. de Gregorio-Monsalvo, J. F. Gomez, O. Suarez, T. B. H. Kuiper,L. F. Rodriguez and E. Jimenez-Bailon , Astrophys. J. **642**, 319 (2006).

[7] G. Maier and H. P. Reisenauer, in *Carbenes in Matrices: Spectroscopy, Structure and Photochemical Pehaviour, Advances in Carbene Chemistry, Vol. 3*, edited by U. Brinker (Elsevier, Amsterdam, 2001), p. 115.

[8] G. Maier, H. P. Reisenauer and R. Ruppel, Eur. J. Org. Chem. 4197 (2004).

[9] H. Wang, J. Szczpanski, A. Cooke, P. Brucat and M. Vala, Int. J. Quantum. Chem. **102**, 806 (2005).

[10] A. J. Schoeffler, H. Kohguchi, K. Hoshima, Y. Ohshima and Y. Endo, J. Chem. Phys. **114**, 6142 (2001).

[11] M. Nakajima, Y. Sumiyoshi and Y. Endo, J. Chem. Phys. **117**, 9327 (2002).

[12] E. Riaplov, M. Wyss, J. P. Maier, D. Panten, G. Chambaud, P. Rosmus and J. Fabian, J. Mol. Spectrosc. **222**, 15 (2003).

[13] S. Lee, Chem. Phys. Lett. **268**, 69 (1997).

[14] G. Pascoli and H. Lavendy, Int. J. Mass. Spectr. Ion Proc. **181**, 11 (1988).

[15] I. Pérez-Juste, A. M. Graña, Luis Carballeira and R. A. Mosquera, J. Chem. Phys. **121**, 10447 (2004).

[16] J. Zhang, W. Wu, L. Wang, and Z. Cao, J. Chem. Phys. **124**, 124319 (2006).

[17] Y. Xie and H. F. Schaefer III, J. Chem. Phys. **96**, 3714 (1992).

[18] Z. -L. Cai, X. -G. Zhang and X. -Y. Wang, Chem. Phys. Lett. **213**, 168 (1993).

[19] J. T. Hougen, J. Chem. Phys. **36**, 519 (1962).

[20] G. Herzberg, *Molecular Spectra and Molecular Structure. III. Electronic Spectra and Electronic Structure of Polyatomic Molecules* (Van Nostrand, Princeton (NJ), 1967).

[21] S. Carter, N. C. Handy, C. Puzzarini, R. Tarroni and P. Palmieri, Mol. Phys. **98**, 1697 (2000).

[22] R. Tarroni, A. Mitrushenkov, P. Palmieri, and S. Carter, J. Chem. Phys. **115**, 11200 (2001).

[23] M. Biczysko, R. Tarroni, and S. Carter, J. Chem. Phys. **119**, 4197 (2003).

[24] R. Tarroni, Chem. Phys. Lett. **380**, 624 (2003).

[25] R. Tarroni and S. Carter, J. Chem. Phys. **119**, 12878 (2003).

[26] R. Tarroni and S. Carter, Mol. Phys. **102**, 2167 (2004).

[27] R. Tarroni and S. Carter, J. Chem. Phys. **123**, 014320 (2005).

[28] R. Tarroni and S. Carter, Mol. Phys. **104**, 2821 (2006).

[29] S. Carter, N. C. Handy, and R. Tarroni, Mol. Phys. **103**, 1131 (2005).

[30] MOLPRO is a package of *ab initio* programs written by H. J. Werner and P. J. Knowles, with contributions of R.D. Amos, A. Bernhardsson, A. Berning, P. Celani, D.L. Cooper, M. J. O. Deegan, A. J. Dobbyn, F. Eckert, C. Hampel, G. Hetzer, T. Korona, R. Lindh, A. W. Lloyd, S. J. McNicholas, F. R. Mamby, W. Meyer, M. E. Mura, A. Nicklass, P. Palmieri, R. Pitzer, G. Rauhut, M. Schütz, H. Stöll, A. J. Stone, R. Tarroni and T. Thorsteinsson.

[31] H. J. Werner and P. J. Knowles, J. Chem. Phys. **89**, 5803 (1988).

[32] P. J. Knowles and H. J. Werner, Chem. Phys. Lett. **145**, 514 (1988).

[33] T. H. Dunning, Jr., J. Chem. Phys. **90**, 1007 (1989).

[34] W. Domcke and C. Woywod, Chem. Phys. Lett. **216**, 362 (1993).

[35] H. J. Werner and P. J. Knowles, J. Chem. Phys. **82**, 5053 (1985).

[36] P.J. Knowles and H.J. Werner, Chem. Phys. Lett. **115**, 259 (1985).

[37] T. Pacher, L. S. Cederbaum, and H. Köppel, J. Chem. Phys. **89**, 7367 (1988).

[38] T. Pacher, L. S. Cederbaum, and H. Köppel, Adv. Chem. Phys. **84**, 293 (1993).

[39] J. Senekowitsch, Ph.D. Thesis, Frankfurt, (1988).

Table 1. Expansion coefficients of the three diabatic energy surfaces ($V_{\Sigma^-}, V_{\Pi^-}, V_{\Pi^+}$) and of the coupling potential (V_{12}) All coefficients are in E_h (hartree) units. The corresponding reference geometries (bohr, rad) of the four surfaces are reported at the bottom of the table. The V_ξ potentials are expressed as simple sums of terms: $V_\xi(q_1,q_2,q_3) = \sum_{ijk} C^\xi_{ijk}\ q_1^i\ q_2^j\ q_3^k$, while for the V_{12} coupling potential the modified expansion: $V_{12}(q_1,q_2,q_3) = \sin q_3(1-\tanh q_1)(1-\tanh q_2)\sum_{ijk} C^{12}_{ijk}\ q_1^i\ q_2^j\ q_3^k$ was used instead. The q_1, q_2, q_3 coordinates are defined as: $q_1 = R_{CC} - R^{ref}_{CC}$, $q_2 = R_{CS} - R^{ref}_{CS}$, $q_3 = \theta - \theta^{ref}$ (radiants), R_{CC}, R_{CS} and θ being the CC, CS and ∠CCS bond lengths and bond angle. The values enclosed in parentheses are empirically adjusted coefficients used to perform variational computations. See text for details.

i	j	k	$C^{\Sigma^-}_{ijk}$	$C^{\Pi^-}_{ijk}$	$C^{\Pi^+}_{ijk}$	C^{12}_{ijk}	i	j	k	$C^{\Sigma^-}_{ijk}$	$C^{\Pi^-}_{ijk}$	$C^{\Pi^+}_{ijk}$	C^{12}_{ijk}
0	0	0	0.000000	0.041665	0.041665	0.046799							
				(0.0409)	(0.0409)	(0.0471)	1	0	6	0.000000	0.000000	0.000000	0.079409
0	0	2	0.066412	0.038739	0.056543	0.003425	1	1	0	0.033719	0.078423	0.078423	0.097170
0	0	4	0.012229	-0.025263	-0.028896	-0.018849	1	1	2	-0.021197	0.034575	-0.039532	-0.015475
0	0	6	-0.039264	0.025448	0.021409	0.012960	1	2	0	-0.023180	-0.034991	-0.034991	0.047880
0	0	8	0.016152	0.000000	0.000000	0.000000	1	3	0	0.001522	-0.015409	-0.015409	0.023767
0	1	0	0.000000	0.000000	0.000000	0.026204	2	0	0	0.268935	0.377216	0.377216	0.102548
0	1	2	-0.056922	-0.045967	-0.057161	-0.012352	2	0	2	-0.011252	-0.013451	0.015320	-0.050736
0	2	0	0.229940	0.175084	0.175084	0.023200	2	1	0	0.003060	-0.022011	-0.022011	0.069673
0	2	2	0.020416	0.016802	0.014359	-0.011573	2	2	0	0.011148	0.040183	0.040183	-0.067217
0	3	0	-0.231998	-0.182997	-0.182997	0.005255	3	0	0	-0.309601	-0.427844	-0.427844	0.074522
0	4	0	0.143525	0.123253	0.123253	0.012273	3	1	0	-0.010836	-0.028667	-0.028667	-0.042011
0	5	0	-0.069369	-0.059496	-0.059496	-0.032297	4	0	0	0.200193	0.298305	0.298305	0.028171
0	6	0	0.020438	0.016376	0.016376	0.000000	5	0	0	-0.112229	-0.145702	-0.145702	0.000000
1	0	0	0.000000	0.000000	0.000000	0.103701	6	0	0	0.056141	0.037648	0.037648	0.000000
1	0	4	0.000000	0.000000	0.000000	-0.123010							
1	0	2	0.041919	-0.083931	-0.016274	0.012089							
R^{ref}_{CC}			2.493245	2.356579	2.356579	2.493245							
R^{ref}_{CS}			2.970580	3.054988	3.054988	2.970580							
θ^{ref}			π	π	π	π							

Table 2. Calculated and experimental energy levels (cm^{-1}) of the $X^3\Sigma^-$ state. Only levels with $v_1 + v_2 + v_3 \leq 4$ are reported, with v_1, v_3 quantum numbers corresponding to the Q_1 and the Q_3 stretching coordinates and v_2 corresponding to the bending coordinate. The value in parenthesis is the fractional contribution of the diabatic $^3\Sigma^-$ component to the total wavefunction.

(v_1, v_2, v_3)Symmetry	Calculated	Experimental[a]
$(010)^3\Pi$	268 (0.95)	266.6
$(020)^3\Sigma$	540 (0.93)	532.8
$(030)^3\Pi$	815 (0.92)	797.9
$(040)^3\Sigma$	1090 (0.90)	
$(001)^3\Sigma$	850 (0.98)	857.8, 862.7[b], 857.2[c]
$(011)^3\Pi$	1125 (0.95)	
$(021)^3\Sigma$	1404 (0.93)	
$(031)^3\Pi$	1685 (0.92)	
$(002)^3\Sigma$	1701 (0.97)	1716.2
$(012)^3\Pi$	1982 (0.95)	1995.8
$(022)^3\Sigma$	2267 (0.93)	2270.0
$(003)^3\Sigma$	2550 (0.97)	2570.1
$(013)^3\Pi$	2838 (0.95)	
$(004)^3\Sigma$	3398 (0.97)	3424.7
$(100)^3\Sigma$	1661 (0.97)	1670.8, 1666.6[b], 1662.6[c]
$(110)^3\Pi$	1922 (0.95)	1932.1
$(120)^3\Sigma$	2189 (0.92)	2191.3
$(130)^3\Pi$	2457 (0.90)	2449.3
$(200)^3\Sigma$	3298 (0.97)	3318.4, 3311.1[b]
$(210)^3\Pi$	3557 (0.95)	
$(220)^3\Sigma$	2189 (0.93)	
$(300)^3\Sigma$	4959 (0.97)	
$(310)^3\Pi$	5240 (0.95)	
$(400)^3\Sigma$	6610 (0.98)	
$(101)^3\Sigma$	2494 (0.97)	2511.6
$(111)^3\Pi$	2765 (0.95)	2763.4[b]
$(121)^3\Sigma$	3039 (0.93)	
$(102)^3\Sigma$	3332 (0.97)	3354.4
$(112)^3\Pi$	3609 (0.95)	
$(201)^3\Sigma$	4169 (0.97)	
$(211)^3\Pi$	4455 (0.95)	
$(202)^3\Sigma$	4923 (0.97)	
$(301)^3\Sigma$	5795 (0.97)	

[a] Ref.[10], unless otherwise indicated. [b] Ref. [8]. [c] Ref. [9].

Table 3. Calculated band origins (cm^{-1}) for the $A^3\Pi$ electronic system of CCS. Only levels with $v_1 + v_2 + v_3 \leq 4$ and $K \leq 1$ are reported, together with the amount of Π contribution to the total wavefunction. Tentative assignments are marked with a question mark close to the experimental value

$(v_1v_2v_3)$	Label	Calculated	Experimental
(000)	$^3\Pi_2$	9106 (0.99)	9146[a]
	$^3\Pi_1$	9239 (0.98)	9249[a]
	$^3\Pi_0$	9370 (0.93)	9442[a]
(010)	$\mu^3\Sigma_1$	9551 (0.98)	
	$\mu^3\Sigma_0$	9624 (1.00)	
	$\kappa^3\Sigma_0$	9786 (0.85)	
	$\kappa^3\Sigma_1$	9857(0.49) 9861(0.43)	
(020)	$\mu^3\Pi_2$	9998 (0.98)	
	$\mu^3\Pi_0$	9997 (0.98)	
	$\mu^3\Pi_1$	10065 (0.99)	
	$\kappa^3\Pi_1$	10281 (0.83)	
	$\kappa^3\Pi_0$	10333 (0.88)	
	$\kappa^3\Pi_2$	10340 (0.87)	
(030)	$\mu^3\Sigma_1$	10428 (0.99)	
	$\mu^3\Sigma_0$	10480 (1.00)	
	$\kappa^3\Sigma_0$	10774 (0.71)	
	$\kappa^3\Sigma_1$	10817(0.59) 10826(0.36)	
(040)	$\mu^3\Pi_2$	10861 (0.94)	
	$\mu^3\Pi_0$	10863 (0.94)	
	$\mu^3\Pi_1$	10910 (1.00)	
	$\kappa^3\Pi_1$	11249(0.42) 11255(0.50)	
	$\kappa^3\Pi_0$	11280 (0.68)	11278.4[b]
	$\kappa^3\Pi_2$	11286(0.35) 11295(0.52)	
(001)	$^3\Pi_2$	9894 (0.98)	
	$^3\Pi_1$	10019 (0.98)	
	$^3\Pi_0$	10160 (0.94)	

$(v_1v_2v_3)$	Label	Calculated	Experimental
(011)	$\mu^3\Sigma_1$	10327 (0.95)	
	$\mu^3\Sigma_0$	10394 (1.00)	
	$\kappa^3\Sigma_0$	10572 (0.74)	
	$\kappa^3\Sigma_1$	10642 (0.73)	
(021)	$\mu^3\Pi_2$	10759 (0.96)	
	$\mu^3\Pi_0$	10760 (0.98)	
	$\mu^3\Pi_1$	10830 (0.97)	
	$\kappa^3\Pi_1$	11058 (0.82)	
	$\kappa^3\Pi_0$	11101(0.35) 11117(0.58)	
	$\kappa^3\Pi_2$	11123 (0.69)	
(031)	$\mu^3\Sigma_1$	11176 (0.99)	
	$\mu^3\Sigma_0$	11225 (1.00)	
	$\kappa^3\Sigma_0$	11543(0.55) 11549(0.40)	
	$\kappa^3\Sigma_1$	11591 (0.68)	
(002)	$^3\Pi_2$	10673 (0.95)	
	$^3\Pi_1$	10787 (0.85)	
	$^3\Pi_0$	10943 (0.95)	
(012)	$\mu^3\Sigma_1$	11094 (0.97)	
	$\mu^3\Sigma_0$	11152 (1.00)	
	$\kappa^3\Sigma_0$	11343 (0.47)	
	$\kappa^3\Sigma_1$	11426 (0.56)	
(022)	$\mu^3\Pi_2$	11509 (0.95)	
	$\mu^3\Pi_0$	11511 (0.97)	
	$\mu^3\Pi_1$	11587(0.58) 11588(0.49)	
	$\kappa^3\Pi_1$	11838 (0.82)	
	$\kappa^3\Pi_0$	11887 (0.70)	
	$\kappa^3\Pi_2$	11896 (0.80)	

Table 3. Continued.

$(v_1v_2v_3)$	Label	Calculated	Experimental
(003)	$^3\Pi_2$	11443 (0.90)	11452.8^b ?
	$^3\Pi_1$	11538 (0.88)	
	$^3\Pi_0$	11719 (0.94)	11716.8^b ?
(013)	$\mu^3\Sigma_1$	11850 (0.91)	
	$\mu^3\Sigma_0$	11894 (1.00)	
	$\kappa^3\Sigma_0$	12118 (0.59)	
	$\kappa^3\Sigma_1$	12186(0.43) 12190(0.44) 12197(0.34)	
(004)	$^3\Pi_2$	12203 (0.94)	
	$^3\Pi_1$	12334 (0.99)	
	$^3\Pi_0$	12483 (0.95)	
(100)	$^3\Pi_2$	10925 (0.89)	10986^a 10925.4^b
	$^3\Pi_1$	11063 (0.82)	11079^a 11056.3^b
	$^3\Pi_0$	11197 (0.81)	11268^a 11191.9^b
(110)	$\mu^3\Sigma_1$	11369(0.40) 11377(0.52)	
	$\mu^3\Sigma_0$	11447 (1.00)	
	$\kappa^3\Sigma_0$	11599(0.31) 11609(0.38) 11610(0.26) 11627(0.30)	11545.2^b
	$\kappa^3\Sigma_1$	11684 (0.85)	$11636^{a,d}$ 11614.3^b
(120)	$\mu^3\Pi_2$	11820 (0.82)	
	$\mu^3\Pi_0$	11824 (0.69)	
	$\mu^3\Pi_1$	11876(0.44) 11897(0.47)	11983^b
	$\kappa^3\Pi_1$	12105(0.43) 12115(0.42)	12001.1^b
	$\kappa^3\Pi_0$	12157 (0.81)	
	$\kappa^3\Pi_2$	12160 (0.80	
(130)	$\mu^3\Sigma_1$	12245(0.51) 12255(0.34)	
	$\mu^3\Sigma_0$	12304 (1.00)	
	$\kappa^3\Sigma_0$	12602 (0.50)	
	$\kappa^3\Sigma_1$	12638 (0.85)	
(200)	$^3\Pi_2$	12732 (0.94)	12795^a 12737.0^b
	$^3\Pi_1$	12863 (0.97)	12882^a 12857.5^b
	$^3\Pi_0$	12996 (0.98)	13081^a 13004.7^b
(210)	$\mu^3\Sigma_1$	13172 (0.94)	
	$\mu^3\Sigma_0$	13249 (1.00)	
	$\kappa^3\Sigma_0$	13402 (0.70)	13342.4^b 13350.8^b 13356.4^b
	$\kappa^3\Sigma_1$	13473 (0.96)	13417.4^b
(220)	$\mu^3\Pi_2$	13616 (0.98)	
	$\mu^3\Pi_0$	13623 (0.98)	
	$\mu^3\Pi_1$	13693 (0.98)	
	$\kappa^3\Pi_1$	13883 (0.91)	
	$\kappa^3\Pi_0$	13945 (0.94)	
	$\kappa^3\Pi_2$	13941 (0.94)	
(300)	$^3\Pi_2$	14508 (0.99)	14542.0^b
	$^3\Pi_1$	14631 (0.98)	14660.2^b
	$^3\Pi_0$	14772 (0.98)	14786.7^b
(310)	$\mu^3\Sigma_1$	14948 (0.99)	
	$\mu^3\Sigma_0$	15034 (1.00)	
	$\kappa^3\Sigma_0$	15117(0.67) 15120(0.44) 15155(0.82)	15131.1^b 15138.1^b 15144.9^b
	$\kappa^3\Sigma_1$	15232(0.76) 15234(0.58)	15217.3^b

Table 3. Continued.

$(v_1v_2v_3)$	Label	Calculated	Experimental
(400)			
	$^3\Pi_2$	16248(0.95) 16249(0.91)	
	$^3\Pi_1$	16377 (0.91)	16420[c]
	$^3\Pi_0$	16523(0.96) 16525(0.95)	
(101)			
	$^3\Pi_2$	11707 (0.77)	
	$^3\Pi_1$	11851 (0.60)	11858.8[b] ?
	$^3\Pi_0$	11995 (0.89)	11983.6[b] ?
(111)			
	$\mu^3\Sigma_1$	12147 (0.77)	
	$\mu^3\Sigma_0$	12217 (1.00)	
	$\kappa^3\Sigma_0$	12412 (0.74)	12331.4[b]
	$\kappa^3\Sigma_1$	12474 (0.92)	
(121)			
	$\mu^3\Pi_2$	12577 (0.66)	
	$\mu^3\Pi_0$	12579 (0.69)	
	$\mu^3\Pi_1$	12614 (0.55)	
	$\kappa^3\Pi_1$	12895 (0.82)	12814.6[b]
	$\kappa^3\Pi_0$	12937(0.88) 12947(0.92)	12907.8[b]
	$\kappa^3\Pi_2$	12947 (0.90)	
(102)			
	$^3\Pi_2$	12502 (0.96)	
	$^3\Pi_1$	12658 (0.98)	
	$^3\Pi_0$	12770(0.44) 12773(0.62)	12770.3[b] ?
(112)			
	$\mu^3\Sigma_1$	12996 (0.95)	
	$\mu^3\Sigma_0$	13049 (1.00)	
	$\kappa^3\Sigma_0$	13175 (0.80)	
	$\kappa^3\Sigma_1$	13236 (0.64)	

$(v_1v_2v_3)$	Label	Calculated	Experimental
(201)			
	$^3\Pi_2$	13524 (0.98)	13535.2[b]
	$^3\Pi_1$	13640 (0.83)	13671.9[b]
	$^3\Pi_0$	13795 (0.93)	13802.9[b] ? 13804.7[b] ?
(211)			
	$\mu^3\Sigma_1$	13951 (0.99)	
	$\mu^3\Sigma_0$	14021 (1.00)	
	$\kappa^3\Sigma_0$	14188 (0.91)	
	$\kappa^3\Sigma_1$	14265 (0.83)	
(202)			
	$^3\Pi_2$	14304 (0.99)	
	$^3\Pi_1$	14461 (0.97)	
	$^3\Pi_0$	14579 (0.94)	
(301)			
	$^3\Pi_2$	15298 (0.98)	15318.3[b] ?
	$^3\Pi_1$	15432 (0.92)	15475.5[b]
	$^3\Pi_0$	15571 (0.98)	

[a] Ref. [12]

[b] Ref. [11]

[c] Ref. [10]

[d] Assigned as a component of the (101) state in Ref.[12]

FIGURE CAPTIONS

Figure 1 Contour plots of the PES's at linear geometries for the lowest $^3\Sigma^-(1^3A'')$ (gray) and $^3\Pi(2^3A'', 1^3A')$ (black) electronic states of C_2S. Energy increments of 1000 cm^{-1} are shown, starting from the minimum of the $^3\Sigma^-$ state. The crossing seam is shown as a bold line and the black diamonds indicate the geometries selected for the *ab initio* computations.

Figure 2 Calculated energy levels of C_2S radical between 9000 and 10000 cm^{-1}, for $J = 0 - 3$ total angular momentum. Levels with a dominant "Π" character state are highlighted and marked with the labels appropriate for the vibronic levels of a triplet Renner-Teller system [20]

Figure 3 Graphical representation of the energy levels reported in Table 3, (solid lines) grouped according their vibronic symmetry. Dashed lines indicate experimental observations taken from Ref.[11].

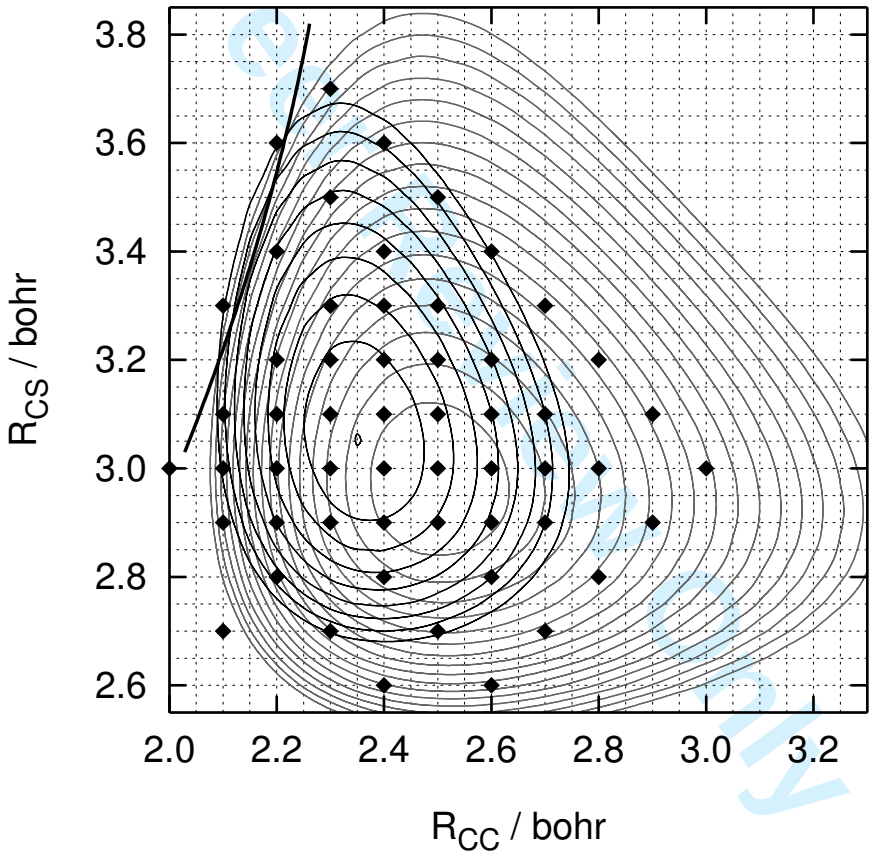

Figure 1 Tarroni et al.

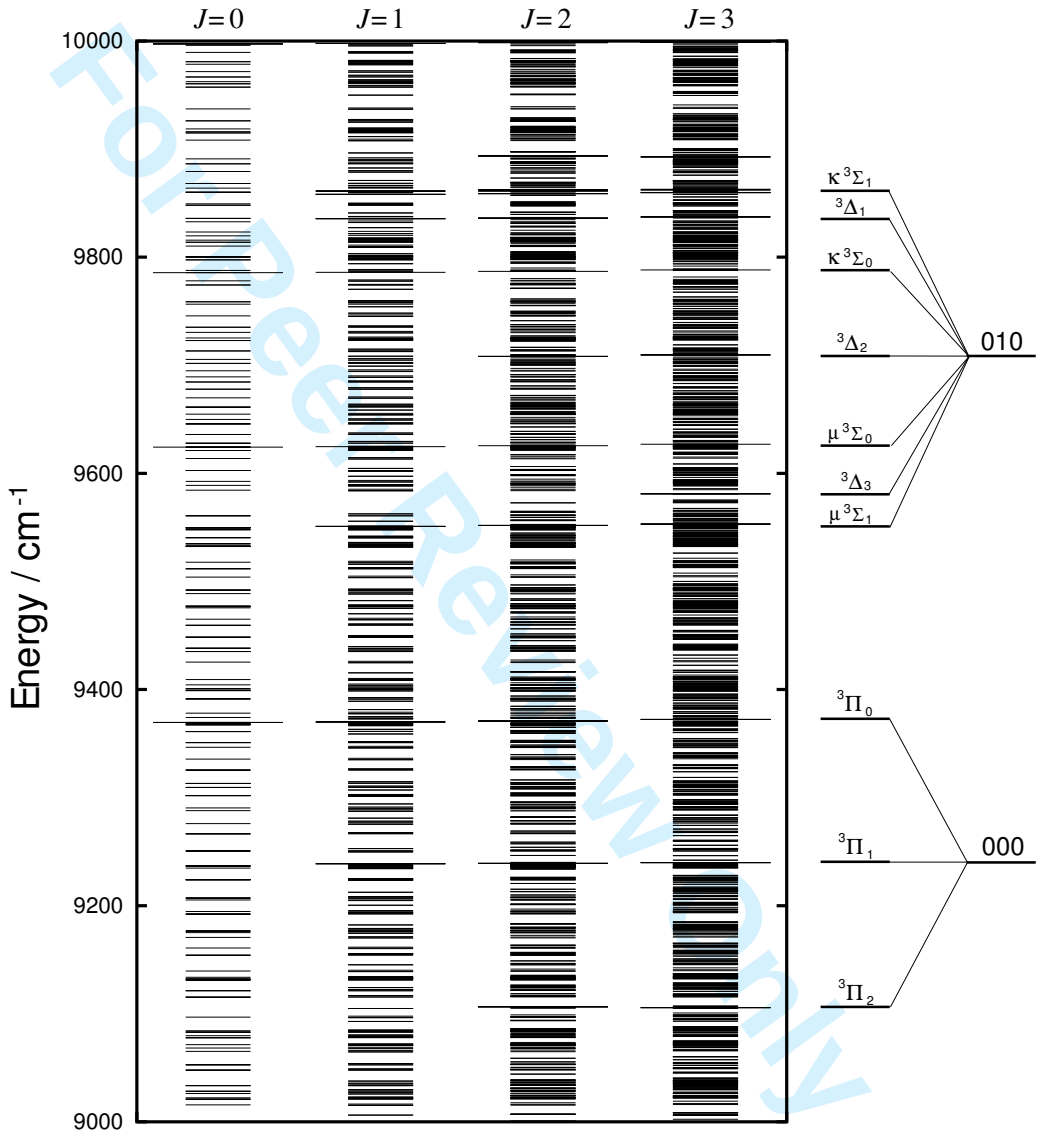

Figure 2 Tarroni et al.

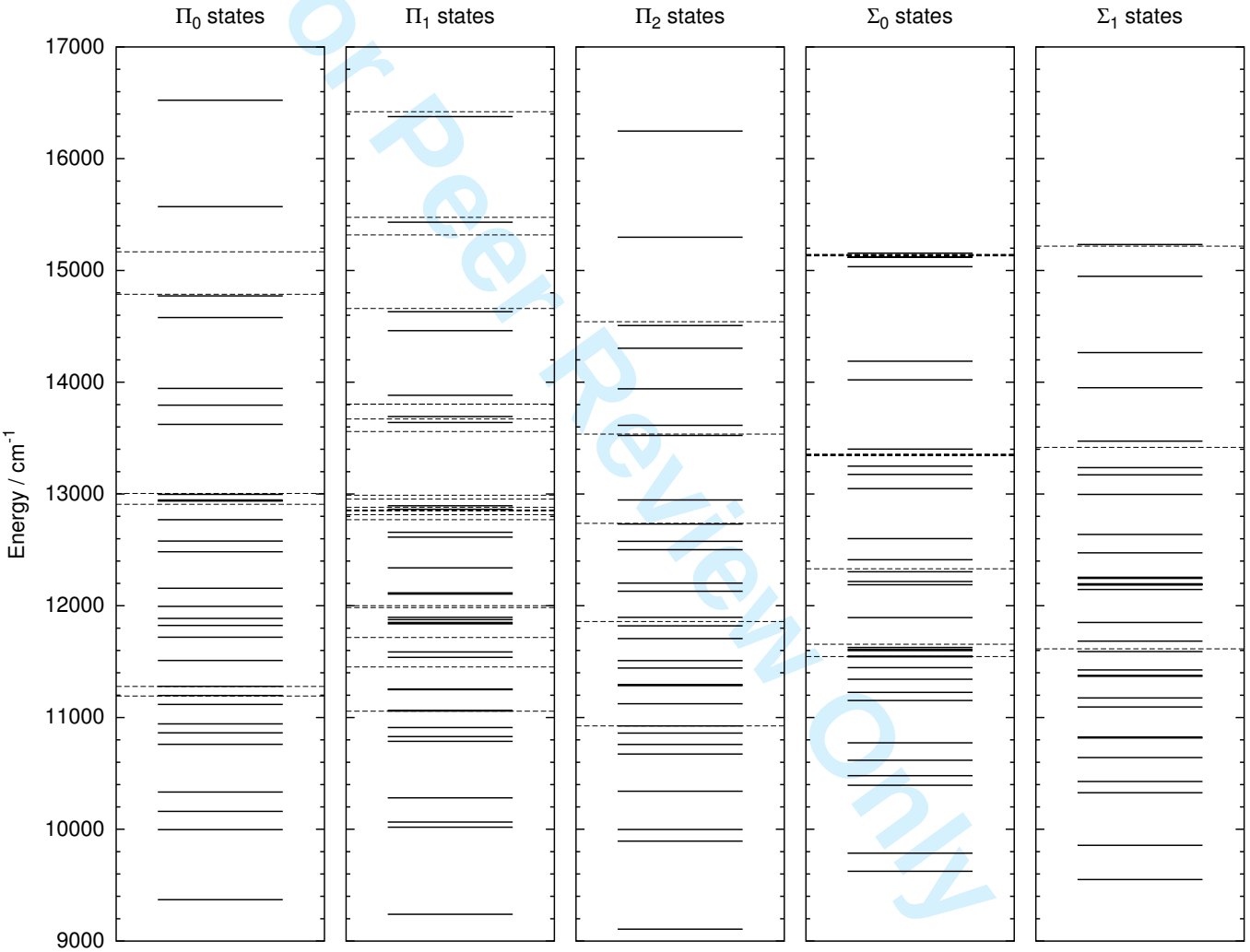

Figure 3 Tarroni et al.